Grazing exit versus grazing incidence geometry for x-ray absorption near edge structure analysis of arsenic traces

F. Meirer,[1,a)] G. Pepponi,[2] C. Streli,[1] P. Wobrauschek,[1] and N. Zoeger[1]
[1]*Atominstitut, Vienna University of Technology, 1020 Wien, Austria*
[2]*Fondazione Bruno Kessler, via Sommarive 18, 38050 Povo (Trento), Italy*

(Received 18 September 2008; accepted 23 February 2009; published online 15 April 2009)

In the presented study the grazing exit x-ray fluorescence was tested for its applicability to x-ray absorption near edge structure analysis of arsenic in droplet samples. The experimental results have been compared to the findings of former analyses of the same samples using a grazing incidence (GI) setup to compare the performance of both geometries. Furthermore, the investigations were accomplished to gain a better understanding of the so called self-absorption effect, which was observed and investigated in previous studies using a GI geometry. It was suggested that a normal incidence-grazing-exit geometry would not suffer from self-absorption effects in x-ray absorption fine structure (XAFS) analysis due to the minimized path length of the incident beam through the sample. The results proved this assumption and in turn confirmed the occurrence of the self-absorption effect for GI geometry. Due to its lower sensitivity it is difficult to apply the GE geometry to XAFS analysis of trace amounts (few nanograms) of samples but the technique is well suited for the analysis of small amounts of concentrated samples. © *2009 American Institute of Physics*. [DOI: 10.1063/1.3106086]

I. INTRODUCTION

A measurement setup utilizing an angle of incidence in the range (plus or minus a few millirad) of the angle of total reflection of x rays is called "grazing incidence" or "glancing incidence" (GI) setup. X-ray fluorescence measurements using angles smaller than the critical angle of total reflection are called total reflection x-ray fluorescence (TXRF) analysis. Therefore the total reflection geometry can be characterized as a special case of grazing incidence measurements. GI x-ray fluorescence (GI-XRF) uses the angle dependent wave field intensity in order to characterize the structure of layered materials and the composition gradient of materials that are inhomogeneous along the direction perpendicular to the surface. The interference between incident and reflected beam causes in case of microcrystalline samples an intensity increase of the fluorescence signal by a factor $(1+R)$, where R is the reflectivity numerically close to 1. The additional effect due to the penetration depth in the nm region is a low background.[1–3]

In contrast to GI-XRF geometry, it is also possible to excite under normal incidence and detect the fluorescence radiation under glancing angles.[1,4–8] This method is called "grazing exit,"[8–11] "grazing emission" (GE-XRF),[5–7,12] or "glancing-takeoff" XRF[13,14] and is theoretically based on the reciprocity theorem.[4] The interference in this case is not between the exciting primary and reflected beam but among the superposition of the "primary" fluorescent waves emitted from the sample and reflected fluorescent radiation when observed under the critical angle of total reflection. This geometry allows surface analysis with adjustable depth penetration equivalent to the GI (or TXRF) setup, according to the reciprocity theorem. A drawback of the GE setup is a lower sensitivity due to the much smaller solid angle seen by the detector. Furthermore absorption of the fluorescence radiation on its way out of the sample due to the sample itself becomes more severe because the path length through the sample is significantly increased. This limits its applicability for quantitative multielemental analysis, as typically carried out in TXRF. An advantage of the GE setup is the possibility to use a focused microbeam of (synchrotron) radiation for excitation. This allows spatially resolved investigations of the sample with the advantage of the surface sensitivity of TXRF. The acquisition of fluorescence radiation in this geometry can be exploited for the measurement of the x-ray absorption and in particular spatially resolved x-ray absorption fine structure (XAFS) studies[15] are feasible. XAFS analysis in GE geometry shows the advantage that the critical angle of total reflection does not change during the energy scan of a XAFS measurement because the interference in GE is not related to the exciting radiation but the fluorescent one, whose energy is constant. Furthermore it was suggested[16,17] that a normal incidence-GE geometry would not suffer from self-absorption effects in XAFS analysis due to the minimized path length of the incident beam through the sample. The self-absorption effect results in a damping of the oscillations (reduced maxima and enhanced minima) of the absorption fine structure and was previously observed when measuring samples with higher elemental concentrations in TXRF geometry.[18–20] It was shown by calculations and measurements that this effect occurs due to the absorption of the incident beam along its path through the sample (which is especially long for TXRF geometry).[19] The path length is equivalent to the penetration depth of the incident beam and is therefore energy dependent. This is the reason why this effect appears for (energy dependent) x-ray absorp-

[a)]Author to whom correspondence should be addressed. Fax: +43/1/58801-141-99. Tel.: +43/1/58801-54-155. Electronic mail: fmeirer@ati.ac.at.

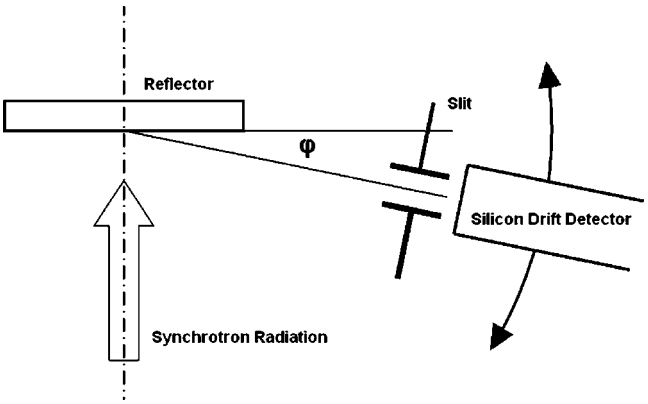

FIG. 1. Sketch of the fundamental arrangement of the experimental setup.

tion near edge structure (XANES) measurements. To reassess that normal-incidence GE geometry does not suffer from this phenomenon, GE experiments have been performed using the same samples that have already been analyzed in TXRF geometry.[19] The performance of the GE setup has been investigated with respect to the following points:

- detection limits (in comparison to TXRF),
- mapping capability,
- XANES measurements (in comparison to TXRF).

II. EXPERIMENTAL

A GE-XRF experiment was performed at HASYLAB beamline L using the newly designed equipment from the Atominstitut Vienna x-ray group. The setup utilizes the fact that silicon drift detectors are lightweight and can therefore be easily moved by translation stages. This makes it possible to fix the sample position and keep the angle of incident (90°) constant during an angle scan. In Fig. 1, the setup and the fundamental arrangement is shown. The setup was designed with the axis of rotation of the detector exactly in the plane of the reflector. A sample holder was constructed to mount this reflector in a precise geometry. Easy sample changing by a motorized translation stage was available. The samples were dried droplets prepared after pipetting a few microliters of a solution in the center of the reflector. A Peltier-cooled Si drift detector with 50 mm^2 active area (Radiant)[21] was used to collect the emitted fluorescence radiation under grazing angles. The detectors effective area of collection was delimited by the slit width (40 or 200 μm) of the defining diaphragm in front of the detector and was therefore roughly 40 $\mu m \times 8$ mm or 200 $\mu m \times 8$ mm.

The angle and the angular divergence of the fluorescence beam were defined by the slit width of the diaphragm and the distance between detector entrance slit and sample (40 mm). These dimensions gave a theoretical angular resolution of 1 mrad (40 μm slit width) or 5 mrad (200 μm slit width). The dimensions of the incident beam of synchrotron radiation were set to 1600×2500 μm^2 (horizontal $\times$ vertical) by a cross-slit system to assure that the whole sample was illuminated. In order to perform measurements with higher lateral resolution, a polycapillary half lens was used to produce a beam spot of 40 μm in diameter.

All measurements were performed in air. Therefore the silicon signal of the reflectors could not be detected because it was absorbed on the relatively long distance (40 mm) between sample and detector. A Si(111) double crystal monochromator was used for selecting the energy of the exciting beam from the continuous x-ray spectrum emitted by the 1.2 Tesla bending magnet at beamline L. The incident x-ray intensity was monitored with an ionization chamber.

A. Samples

Three samples with different total amounts of arsenic masses on quartz reflectors (20 ng, 100 ng) and a Silicon reflector (500 ng) stemming from the sample series already analyzed with TXRF-XANES and characterized using a confocal microscope[19] have been investigated. The samples have been prepared by depositing with a micropipette 1 μl of standard solution and drying under vacuum. More details can be found in Ref. 19.

Additionally a germanium reflector was used to perform angle scans (the silicon signal could not be used due to the absorption in air). This was done to compare the experimental results of the angular scans with theory.

B. GE measurements

Four kinds of measurements have been performed using the GE setup which are as follows.

(1) Angular scans of arsenic samples and germanium reflector using both the unfocused and the focused beam (40 μm beam spot). The angle increments and the lifetime (LT) for each point of the scan were 0.44 mrad and 10 s for the scans using the unfocused beam and 0.22 mrad and 20 s for the scans using the focused beam.
(2) Single TXRF spectra (LT 100 s) of the samples (unfocused beam; 200 μm slit width).
(3) Area scans of the samples using the polycapillary half lens (40 μm beam spot) and the 40 μm entrance slit in front of the detector.
(4) XANES measurements of the arsenic samples (unfocused beam, 200 μm slit width, two of the samples additionally with 40 μm beam spot and 40 μm entrance slit).

Angle dependent measurements were carried out by rotating the detector around the arsenic droplet sample in the center of the reflector. The results of the angular scans were used to adjust an exit angle below the critical angle of total reflection in order to record single spectra, perform XANES measurements, and accomplish the area scans.

For quantification the single fluorescence spectra recorded at 12200 eV have been evaluated using the QXAS (quantitative x-ray analysis system) software package.[22] The limits of detection for 1000 s measurement time (LD_{1000}) have been determined according to

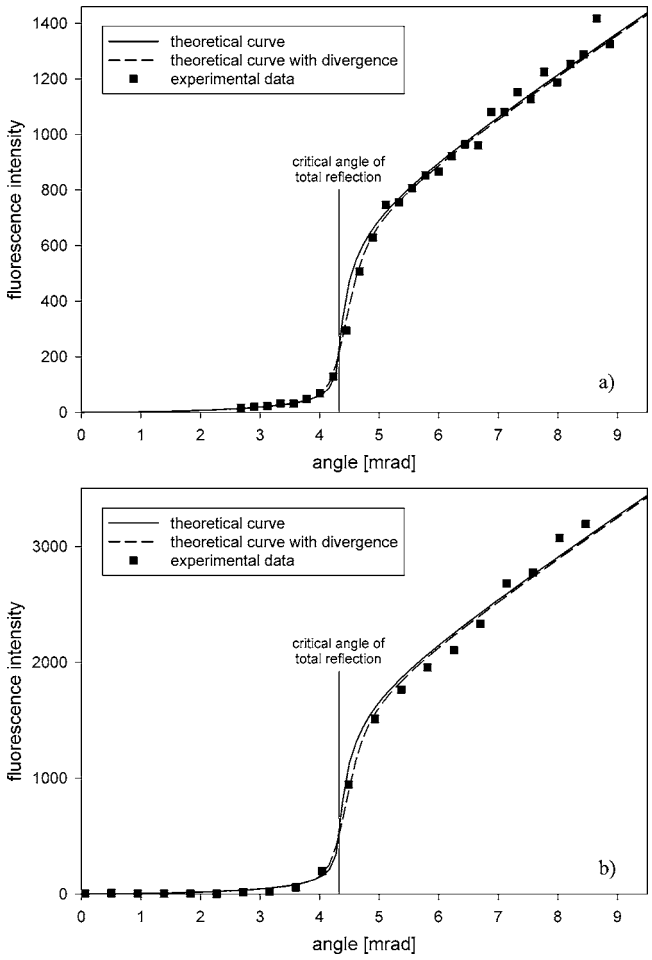

FIG. 2. Angular dependence of the fluorescence intensity of the bulk germanium sample. In (a) the results of the measurements using the focused beam (40 μm spot size) are shown. The data obtained using the unfocused beam is shown in (b). Both measurements were performed using the 40 μm slit in front of the detector. The vertical line indicates the critical angle of total reflection at 4.33 mrad.

$$\mathrm{LD}_{1000} = \frac{3\sqrt{N_B}}{N_N} m_{\mathrm{sample}} \frac{\sqrt{t}}{\sqrt{1000}}, \tag{1}$$

where N_N and N_B are the netto- and background counts of the signal, m_{sample} is the sample mass, and t is the measurement time.

To perform the XANES measurements, the excitation energy was tuned in varying steps (from 5 to 0.5 eV) across the arsenic *K*-edge at 11 867 eV and a fluorescence spectrum was recorded for 10 s at each energy. To calibrate the energy of the exciting radiation, the absorption by an elemental gold foil was recorded in transmission mode. The first inflection point (i.e., the first maximum of the derivative spectrum) of the Au metal foil scan was assumed to be 11 918 eV (Au-*L*3 edge).

Measured absorption spectra have been analyzed with ATHENA which is included in the IFEFFIT program package for x-ray absorption spectroscopy analysis.[23–25] Using this software each scan was normalized and its energy scale was corrected with respect to the Au-*L*3 edge. Repetitive scans of the same sample have been merged by calculating the average and standard deviation at each point in the set.

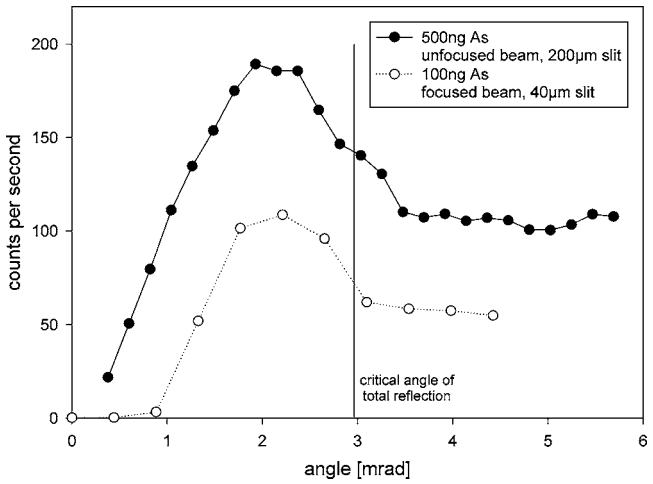

FIG. 3. Angular dependence of the fluorescence intensity of the 100 and 500 ng arsenic samples. The vertical line indicates the critical angle of total reflection at 2.96 mrad.

III. RESULTS AND DISCUSSION

A. Angular scans

Figure 2 shows the results of the angle dependent measurements of the bulk germanium reflector in comparison with the theoretical curves. The data obtained for the angular scan performed with the focused beam (40 μm spot size) and the 40 μm slit in front of the detector is displayed in Fig. 2(a). The second measurement presented in Fig. 2(b) was accomplished using the unfocused beam (1600 $\times$2500 μm^2, horizontal$\times$vertical) and the 40 μm diaphragm. The critical angle of total reflection in GE geometry for germanium was calculated to 4.33 mrad. To estimate the divergence of the measurements the theoretical curve was convolved with a Gaussian function with peak area one. The fit parameter was the full width at half maximum of the Gauss peak. The experimental data and the theoretical curve showed good agreement.

The divergence was expected to be 1 mrad for the measurement with the 40 μm slit. However the divergence determined by the fitting was estimated to be 0.34 mrad for the experiment performed with the focused beam and 0.39 mrad for the angular scan using the unfocused beam. This low divergence can be explained with a misalignment of the slit relative to the reflectors surface. The mentioned effect could have been expected and no effort was spent trying to correct the setup since the higher angular resolution was welcome and the slight loss in sensitivity did not disturb the experiment.

In Fig. 3 the fluorescence signals of the 100 and 500 ng As samples are displayed showing the typical shape with double intensity at angles below the critical angle when compared to larger angles. In GE geometry this effect is caused by the missing contribution due to surface reflections of the fluorescence signal in this region. At 2.96 mrad the theoretically determined critical angle of total reflection in GE geometry for arsenic is indicated. It can be seen that the angular divergence is larger for the scan using the 200 μm diaphragm but is sufficient to determine an angle below the

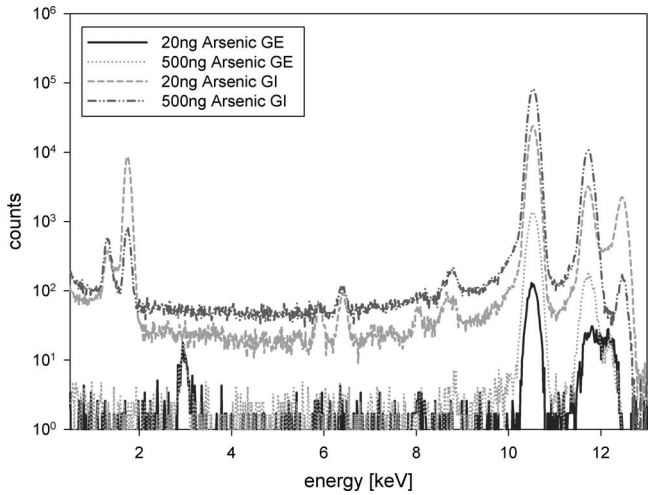

FIG. 4. Comparison of spectra of identical samples recorded for 100 s LT in GE and GI geometry respectively. The GE measurements have been performed in vacuum and the GE spectra were recorded in air. Therefore an argon peak can be seen in the GE spectra while the contribution from the silicon reflector is missing (absorption in air). The excitation energies were 12 200 and 12 500 eV for the GE and GI setup, respectively.

critical angle of total reflection for the further measurements (single TXRF spectra, area scans, and XANES measurements).

B. TXRF spectra

Single spectra have been recorded for 100 s LT for the 20 and 500 ng arsenic samples. The exciting energy was tuned to 12200 eV. Figure 4 shows a comparison of these spectra with spectra recorded for the same samples in GI geometry and at an exciting energy of 12 500 eV.[19] For the calculation of the detection limits (limit of detection, LD) the difference in the exciting energies was not taken into account as the decrease of the photoelectric cross section from 12 200 to 12 500 eV is smaller than 6%. The absorption of the arsenic fluorescence radiation due to the air between sample and detector (distance 40 mm) is smaller than 2% and was therefore also neglected.

Detection limits for the 20 ng arsenic samples were determined by extrapolation for a 1000 s measuring time and found to be 2 pg for the GI geometry and 55 pg a for the GE geometry, respectively. This shows that the sensitivity of the GE setup is one order of magnitude lower than the one of the GI geometry.

C. Area scans

The samples of the series of dried residues with different total amounts of arsenic masses on quartz reflectors (20 ng, 100 ng) and a silicon reflector (500 ng) were scanned with the aid of a polycapillary half lens producing a beam spot of 40 μm in diameter. Figure 5 shows the results of the measurements in comparison with the data obtained with the confocal microscope.[19] All fluorescence intensities are given in counts per second (cps), have been corrected for dead time, and are normalized to 100 mA storage ring current. The scanning parameters are given in Table I. Fluorescence intensities were calculated by region of interest integration because the spectra are practically background free (see Fig. 4). The results show good agreement with the data obtained with the confocal microscope showing the applicability of the GE geometry for spatially resolved analysis.

D. XANES analysis

Experiments were performed with the aim to study XANES self-absorption effects, which were observed previously for the same samples in GI-XRF geometry.[19] Figure 6 shows the results of the XANES measurements performed in GE geometry in comparison with the results of the GI experiments described in.[19] The data has been corrected for dead time and was normalized to the flux of the incident radiation with the aid of an ionization chamber. It can be clearly seen that the samples measured using the GE setup show no damping of the oscillations of the absorption coefficient (within the counting statistics). Damping of the oscillations here refers to the reduced maxima and enhanced minima of the fine structure of the measured absorption coefficient in the GI setup. This phenomenon is particularly effective at the first, strong maximum of the absorption coefficient—the so called "white line"—and is most obvious there. In contrast to that the measurements performed with the GE setup do not show any sample mass dependent changes of the white line and the other fine structure.

The labels 500 ng GE A and 500 ng GE B indicate two independent measurements (sets of repetitive scans), which have been performed to check the influence of the counting statistics. Additionally two samples have been investigated using the focused beam (40 μm spot size). Points of maximum fluorescence intensity found during the area scan of the samples have been chosen for XANES analysis. Figure 7 indicates the positions in the area maps where the XANES scans have been performed. The results of these measurements in comparison with the experiments performed for the same samples using the unfocused beam and the GI geometry are shown in Fig. 8. A small damping of the white line of the scans recorded using the focused beam can be observed. The effect seems to be stronger for the 500 ng sample. As can be observed in the gray scale legend of Fig. 5, the dried spots have a height of 6–18 μm. Considering an As concentration of about 1.25 g/cm^3 in the dried residue[19] and a path length of 10 μm an absorption of about 20% can be estimated at an energy slightly above the edge.[26] This can explain a small self-absorption effect also in the GE experiment. Although the maximum height for the 100 ng sample is larger (18 μm) as can be seen in Fig. 7 the count rate for the measured spots on the two samples are higher for the 500 ng sample and therefore a higher self-absorption can be expected.

IV. CONCLUSIONS

It could be shown that the newly developed GE setup utilizing a movable lightweight silicon drift detector, which allows a fixed sample position works very well for synchrotron radiation induced GE-XRF analysis. Supplementary to some of the advantages of a TXRF analysis in GI geometry [multielement analysis, nondestructive, surface sensitive, and

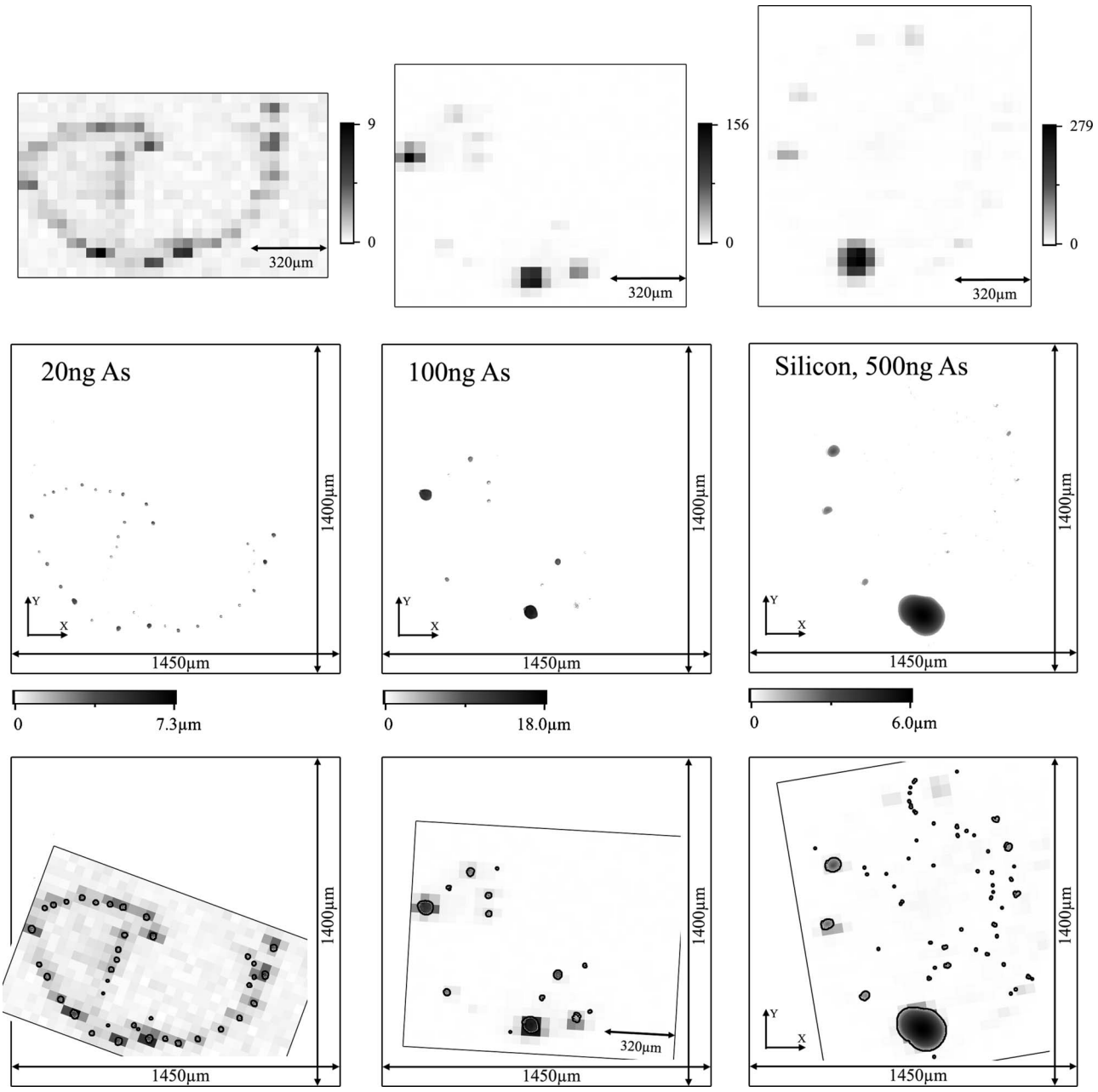

FIG. 5. Area scans of the 20, 100, and 500 ng arsenic samples (first row of maps) in comparison with the results of the measurements with a confocal microscope (second row of maps). The intensities of the fluorescence maps are given in cps, they are dead-time corrected and normalized to 100 mA ring current. The last row of maps shows an overlay of the maps of the first (fluorescence maps) and second row (microscope maps). The fluorescence maps have been slightly rotated to match the microscope images. The spots (representing the sample) of the microscope maps have been encircled in the overlay maps for better visibility. This overlay shows the excellent correlation of the results obtained with the confocal microscope and with micro x-ray fluorescence analysis in GE geometry.

determination of contamination type (residual, surface layer, and bulk)] the GE setup allows the use of a focusing optic for the exciting radiation and it therefore enables spatially resolved investigations of the sample. Angular dependent measurements of bulk and droplet samples as well as area scans of droplet samples with a resolution of 40 μm have been performed showing the advantages of the GE setup.

Detection limits calculated to compare the performance of the GE and the GI arrangement showed that the sensitivity of the GE setup is one order of magnitude lower than the one

TABLE I. Parameters of area scans of all measured samples

Scanning parameters	20 ng As sample	100 ng As sample	500 ng As sample
Pixels (horizontal × vertical)	32 × 19	30 × 25	27 × 30
Step size	40 μm	40 μm	40 μm
Total scanned area	1280 × 760 μm^2	1200 × 1000 μm^2	1080 × 1200 μm^2

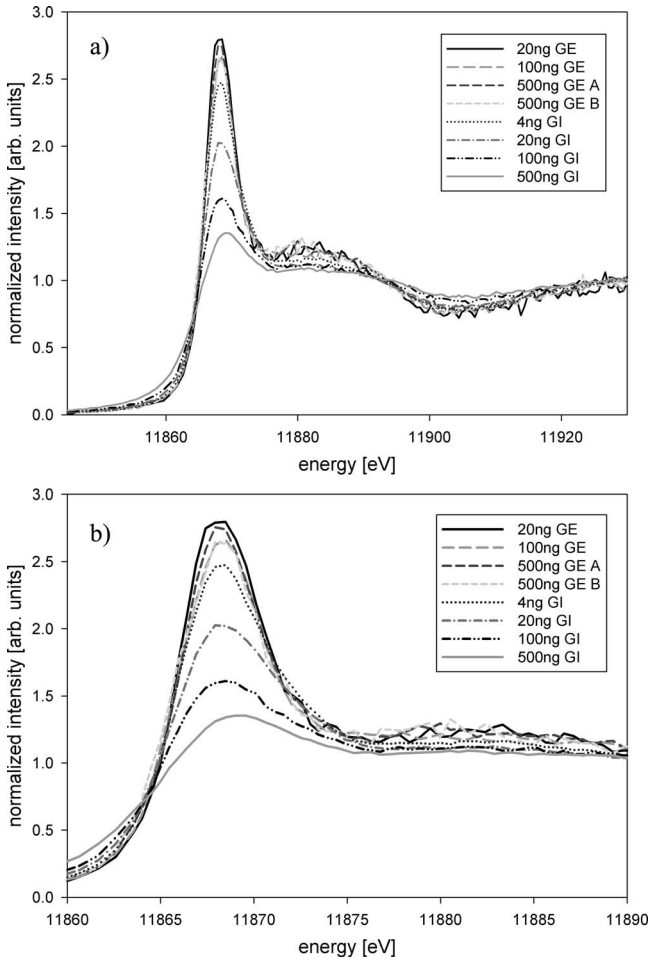

FIG. 6. Comparison of XANES measurements performed for the same samples in GI and GE geometry. In (b) the near edge region is zoomed.

of the GI geometry. Both geometries can be coupled to x-ray absorption spectroscopy to gain information on the chemical state of an element of interest. XANES measurements in GE geometry have been performed and compared with results obtained with a GI arrangement. It could be shown that the GE setup suffers minimally from self-absorption effects which are typical in the GI experiments. Due to the lower sensitivity it is difficult to apply the GE geometry to XAFS analysis of trace amounts (few nanograms) of samples. The self-absorption effect in the GI geometry on the other hand

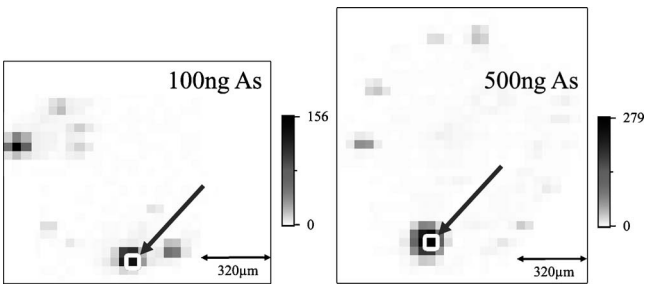

FIG. 7. Points (white circles) chosen for XANES analysis of the 100 and 500 ng arsenic samples using the focused beam. The intensities of the fluorescence maps are given in cps, are dead time corrected and normalized to 100 mA ring current.

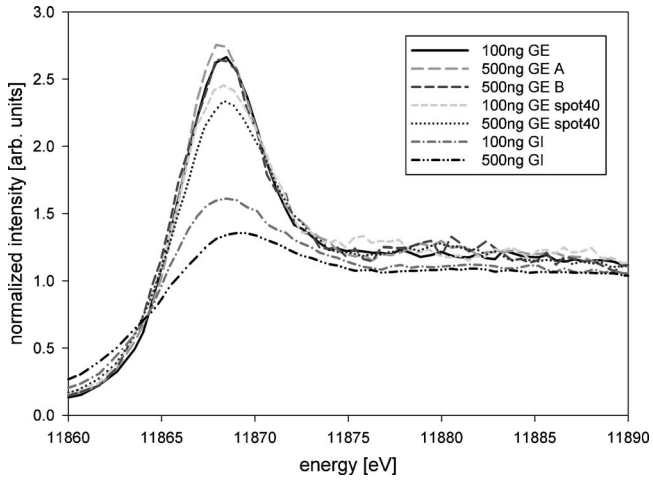

FIG. 8. XANES region of the 100 and 500 ng arsenic samples recorded with different setups. The samples labeled with "GI" have been measured using GI geometry. The rest of the samples were investigated with a GE setup and the curves indicated with "spot40" have been excited by a focused beam with spot size 40 μm.

decreases rapidly with lower sample amounts. Therefore it would be advantageous for a XAFS analysis to measure higher concentrated standard samples in a GE setup and highly diluted samples in GI geometry.

ACKNOWLEDGMENTS

This work was supported by the Austrian Science Fund (FWF) Project No. P18299 and the European Commission Project No. II-20042060.

[1]R. Klockenkämper, *Total Reflection X-Ray Fluorescence Analysis* (Wiley-Interscience, New York, 1997).
[2]P. Wobrauschek, X-Ray Spectrom. **36**, 289 (2007).
[3]C. Streli, P. Wobrauschek, F. Meirer, and G. Pepponi, J. Anal. At. Spectrom. **23**, 792 (2008).
[4]R. S. Becker, J. A. Golovchenko, and J. R. Patel, Phys. Rev. Lett. **50**, 153 (1983).
[5]P. K. de Bokx and H. P. Urbach, Rev. Sci. Instrum. **66**, 15 (1995).
[6]M. Claes, R. Van Grieken, and P. De Bokx, X-Ray Spectrom. **26**, 153 (1997).
[7]R. D. Pérez, H. J. Sánchez, and M. Rubio, X-Ray Spectrom. **30**, 292 (2001).
[8]K. Tsuji, Z. Spolnik, K. Wagatsuma, S. Nagata, and I. Satoh, Anal. Sci. **17**, 145 (2001).
[9]T. Noma, H. Miyata, and S. Ino, Jpn. J. Appl. Phys., Part 2 **31**, L900 (1992).
[10]T. Noma, A. Iida, and K. Sakurai, Phys. Rev. B **48**, 17524 (1993).
[11]T. Noma and A. Iida, Rev. Sci. Instrum. **65**, 837 (1994).
[12]H. J. Sánchez, X-Ray Spectrom. **31**, 145 (2002).
[13]K. Tsuji, K. Wagatsuma, and T. Oku, X-Ray Spectrom. **29**, 155 (2000).
[14]K. Tsuji, S. Sato, and K. Hirokawa, J. Appl. Phys. **76**, 7860 (1994).
[15]A. Iida, X-Ray Spectrom. **26**, 359 (1997).
[16]L. Tröger, D. Arvanitis, K. Baberschke, H. Michaelis, U. Grimm, and E. Zschech, Phys. Rev. B **46**, 3283 (1992).
[17]P. Pfalzer, J. P. Urbach, M. Klemm, S. Horn, M. L. denBoer, A. I. Frenkel, and J. P. Kirkland, Phys. Rev. B **60**, 9335 (1999).
[18]G. Falkenberg, G. Pepponi, C. Streli, and P. Wobrauschek, Spectrochim. Acta, Part B **58**, 2239 (2003).
[19]F. Meirer, G. Pepponi, C. Streli, P. Wobrauschek, P. Kregsamer, N. Zoeger, and G. Falkenberg, Spectrochim. Acta, Part B **63**, 1496 (2008).
[20]F. Meirer, G. Pepponi, C. Streli, P. Wobrauschek, V. G. Mihucz, G. Záray, V. Czech, J. A. C. Broekaert, U. E. A. Fittschen, and G. Falkenberg,

X-Ray Spectrom. **36**, 408 (2007).
[21]www.radiantdetectors.com/vortex.html, the SII Nanotechnology Incorporated Website, 2007.
[22]www.iaea.or.at/programmes/ripc/physics/faznic/qxas.htm, the IAEA homepage, 2008.
[23]http://cars9.uchicago.edu/ifeffit/, the IFEFFIT homepage, 2008.
[24]M. Newville, J. Synchrotron Radiat. **8**, 322 (2001).
[25]B. Ravel and M. Newville, J. Synchrotron Radiat. **12**, 537 (2005).
[26]B. L. Henke, E. M. Gullikson, and J. C. Davis, At. Data Nucl. Data Tables **54**, 181 (1993).